International Journal of Current Research and Modern Education (IJCRME)
Impact Factor: 6.925, ISSN (Online): 2455 - 5428
(www.rdmodernresearch.com) Volume 3, Issue 1, 2018

NUCLEATION KINETICS, METASTABLE ZONE WIDTH AND CHARACTERIZATION OF FERRIC SULFATE DOPED KDP CRYSTALS GROWN BY SLOW EVAPORATION TECHNIQUE

T. Manju* & P. Selvarajan**

***** Research Scholar, Manonmaniam Sundaranar University, Abishekapatti, Tirunelveli, Tamilnadu

** Department of Physics, Aditanar College of Arts and Science, Tiruchendur, Tamilnadu

Cite This Article: T. Manju & P. Selvarajan, "Nucleation Kinetics, Metastable Zone Width and Characterization of Ferric Sulfate Doped KDP Crystals Grown by Slow Evaporation Technique", International Journal of Current Research and Modern Education, Volume 3, Issue 1, Page Number 523-533, 2018.

Abstract:

Undoped and ferric sulfate doped KDP crystals have been grown by solution method with slow evaporation technique. 1 mole% of ferric sulfate was added as the dopant into KDP crystals to alter the various properties of the host KDP crystals. Solubility, metastable zone width and critical nucleation properties were determined for undoped and ferric sulfate doped KDP samples. Solubility is found to be increasing with increase of temperature for both the samples. The crystal structure of the grown crystals was found by XRD method. SHG efficiency was measured for the samples and hardness parameters like Vickers hardness number and work hardening coefficient of the samples were analysed and the hardness is reduced when ferric sulfate was used as the dopant into KDP crystals.

Key Words: KDP, Doping, Solution Growth, Nucleation Kinetics, XRD, SHG, NLO & Microhardness

1. Introduction:

Potassium Dihydrogen Phosphate (KDP) is a negative uniaxial crystal that has a refractive index for extraordinary ray (n_e) along the optic axis and refractive index for ordinary ray (n_o) along the other two axes. KDP crystal is one of the inorganic nonlinear optical (NLO) crystals and it is used as the standard material for second harmonic generation experiments. It is most widely used as a harmonic generator and it is used upto fifth harmonic generation [1-3]. The various physical and chemical properties of KDP have been modified by adding many inorganic and organic dopants by a large number of researchers [4-7]. The impurities like metals ions, amino acids and dyes have been used to alter the properties of KDP crystals [8-10]. The study of the kinetics of KDP crystal growth in the presence of some organic molecules shows that the addition of urea to the mother liquor practically does not influence the growth rate for the faces, whereas ethanol and propanol essentially decrease the growth rate of the faces and lead to their tapering. By studying the influence of urea on the optical, nonlinear and other characteristics of KDP crystals, it is showed that urea doped KDP crystals have a higher mechanical strength and thermal stability in comparison with the pure KDP crystals [11-14]. It is reported that some of the impurities can seriously inhibit the faces of KDP crystals and it can induce the occurrence of secondary nucleation from the growth solutions and thus decrease the solution stability [15-18]. In this work, an attempt can be made to alter the properties of KDP crystals by adding ferric sulfate as the dopant. The aim of the work is to report the nucleation kinetic studies, optical studies, NLO studies and electrical studies of pure and ferric sulfate doped KDP crystals.

2. Experimental Studies:

2.1 Growth of Undoped and Ferric Sulfate Doped KDP Crystals: Analar Reagent (AR) grade chemicals of potassium dihydrogen phosphate (KDP) and ferric sulfate were purchased commercially from Merck India. To grow undoped KDP crystals, 200 ml of saturated solution was prepared using KDP chemical and double distilled water in the growth vessel of 500 ml. The solution was mixed properly and stirred well using a hot plate magnetic stirrer for about 3 hours. Then the solution was filtered and kept in an undisturbed place for slow evaporation. It took about 25-30 days to get the single crystals of KDP. Single crystals of ferric sulfate doped KDP were grown by adding 1 mole% of ferric sulfate into the aqueous solution of KDP. Here also the solution was stirred well for about 3 hours and filtered properly two times. Then the filtered ferric sulfate added KDP solution was taken in a separate growth vessel for crystallization. Both the growth vessels were covered with perforated polythene papers and they were kept in a vibration free platform at room temperature (30 $^{\circ}$C). When the solvent evaporates, it attains supersaturation and nucleation starts and the crystal grows. Seed immersion technique was also adopted to collect big-sized crystals. The grown KDP crystals are observed to be transparent but ferric sulfate doped crystals are found to be slightly transparent. The morphology of ferric sulfate doped KDP crystal is observed to be different when compared to that of the undoped KDP crystal. The presence of impurity in the host KDP crystals is responsible for altering the morphology and transparency. The grown crystals are given in the figure 1.

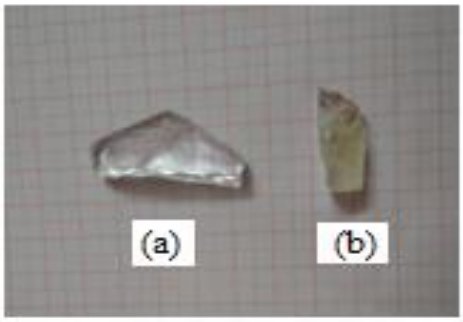

Figure 1: The grown crystals of (a) undoped and (b) ferric sulfate doped KDP crystals

2.2 Solubility, Metastable Zone Width and Crystal Nucleation Kinetics: The solubility of the undoped and ferric sulfate added KDP crystals was determined by gravimetrical method [19]. The powdered sample of KDP was added step by step to 25 ml of double distilled water in an air-tight container kept on the hot plate magnetic stirrer maintaining the temperature at 30°C. After preparing the saturated solution at 30°C, 5ml of the solution was pipetted out and taken in a petri dish and it was warmed up at 45° C till the solvent was evaporated out. By measuring the amount of solute present in the petri dish, the solubility of KDP in double distilled water was determined. The same procedure was followed to find solubility of undoped and ferric sulfate doped KDP samples at other temperatures such as 35, 40, 45, 50, and 60 °C. A constant temperature bath was also used to ascertain the solubility data at various temperatures. Solubility curves for undoped and ferric sulfate doped KDP samples at various temperatures are presented in the figure 2. It is observed from the results that the solubility increases with temperature for both the samples and it is found to be more for ferric sulfate doped KDP than that of undoped KDP sample. As the solubility increases with increase of temperature, the samples have positive temperature coefficient of solubility. Measurement of solubility of samples is necessary to carry out nucleation kinetic studies, finding metastable zone width and to prepare saturated and supersaturated solutions.

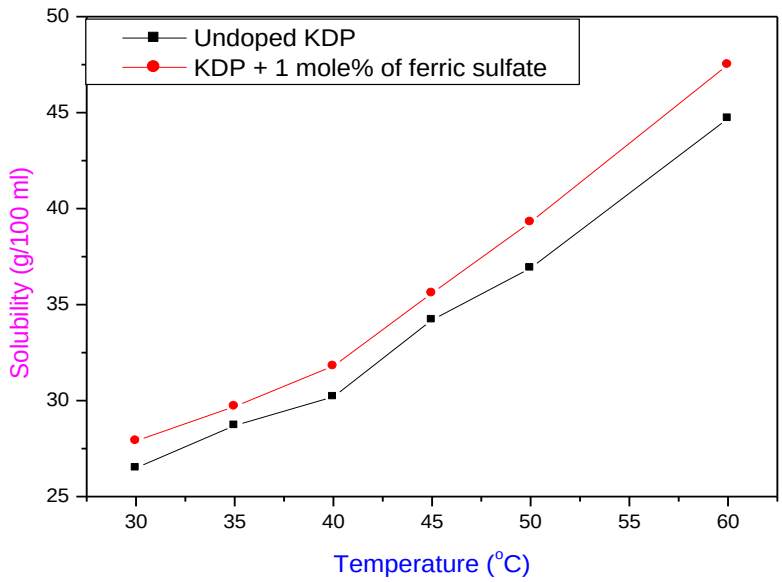

Figure 2: Variation of solubility with temperature for undoped and ferric sulfate doped KDP crystals

A polythermal method was used to find the metastable zone width for the samples [20]. Saturated solution of KDP has been prepared in accordance with the solubility data. The studies were carried out in a constant temperature bath controlled to an accuracy of ±0.01 °C provided with a cryostat for cooling below room temperature. A constant volume of 20 ml of solution was used to find metastable zone width. The solution was slightly pre-heated above the saturated temperature for homogenization and it was cooled from the overheated temperature using the constant temperature bath. The temperature at which the first speck of crystal nucleus is formed in the solution is called the nucleation temperature. This experiment was repeated for the various saturated temperatures at 30, 35, 40, 45 and 50°C. The same procedure was followed to find the metastable zone width for ferric sulfate doped KDP sample. The solubility and the nucleation curves for

undoped and ferric sulfate doped KDP samples are given in the Figs. 3 and 4. The metastable zone width is the difference between the saturation and the nucleation temperatures. It is observed from the results that the metastable zone width is more at low temperature region and it is less when the temperature is more than 40 ^{o}C. When ferric sulfate is added as the dopant into KDP sample, it is found that the metastable zone width is reduced. Usually metastable zone width depends on many parameters like temperature, cooling rate, experimental setup, nature of solution, mechanical effect, presence of impurities and pH value of the solution.

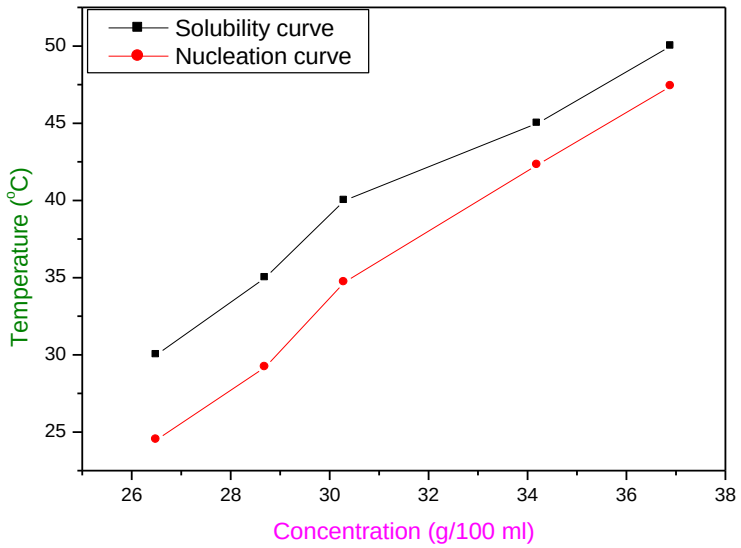

Figure 3: Metastable zone width for undoped KDP sample

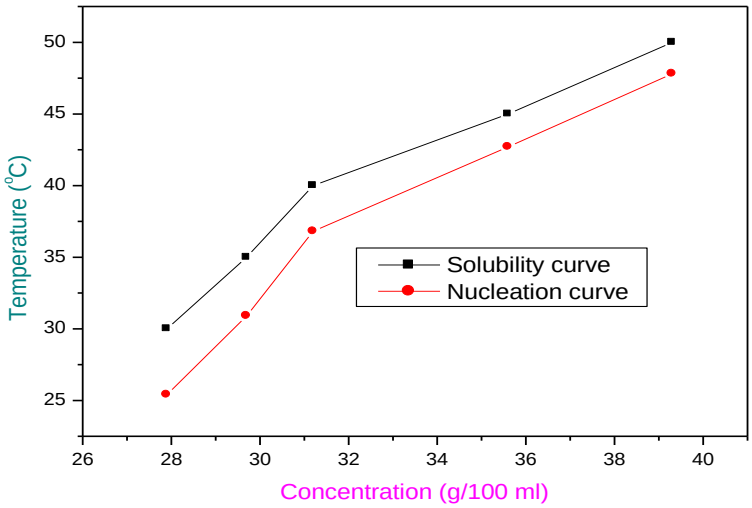

Figure 4: Metastable zone width for ferric sulfate doped KDP sample

Nucleation kinetics reveals valuable information about the crystal growth process, which can be employed in the growth of large size crystals. Since nucleation is the first step towards phase transition, a detailed knowledge about nucleation is of major importance for better control of crystallization or solidification. The classical theory of homogeneous nucleation stems from the thermodynamic approach of Gibbs.

The thermodynamic conditions necessary for a small crystal nucleating homogeneously from solution involve a free energy called Gibbs free energy and is given by $\Delta G = 4\pi r^2\sigma + 4/3\ \pi r^3\Delta G_v$ where r is the radius of the nucleus at the critical state, the driving force for the nucleation from the supersaturated solution is $\Delta G_v = (-kT/V) \ln S$ where σ is the interfacial tension, V is the molar volume of the crystal, T is the absolute temperature of the solution and k is the Boltzmann's constant. Once the nucleation occurs in the supersaturated solution, the nucleus grows quickly and a bright sparkling particle is seen. The time interval in which the observation of the first sparkling particle in the undisturbed supersaturated solution is called the induction period (τ). The expression for the induction period in terms of Gibbs free energy is given by $ln\ \tau = -B + \Delta G / kT$ where B is a

constant, k is the Boltzmann's constant and T is the absolute temperature [21, 22]. The Gibbs free energy will be maximum for a certain value of radius (r^*) of nucleus, which is known as critical radius and the corresponding nucleus is called the critical nucleus. Nuclei formed with radius greater than critical radius are stable and its free energy decreases by growing. The critical radius and the critical energy barrier associated with the critical nucleation are related as $r^*=-2\sigma/\Delta G_v$ and Gibbs free energy change at the critical state is given by $\Delta G^* = mRT / N (\ln S)^2$ or $\Delta G^* = mKT /(\ln S)^2$ where m is the slope of the plot of $1 / (\ln S)^2$ against $\ln \tau$, S is the supersaturation ratio. The interfacial energy can be written as $\sigma = (RT/ N) [3m / 16 \pi v^2]^{1/3}$. Here N k = R where N is the Avogadro's number, R is the universal gas constant.The nucleation rate (*J*) is $J = A \exp(-\Delta G^*/kT)$ where A is the pre-exponential factor. The complete theory of nucleation kinetics can be referred in the literature [23].

For the measurement of induction period, isothermal method was used for the selected supersaturation ratios viz. 1.35, 1.4, 1.45, 1.5 and 1.55 at the constant temperature of 30°C. Using the solubility diagram, the saturated solution of the sample was prepared and taken in a nucleation cell and it was stirred continuously for about 3 hours using a magnetic stirrer to ensure the homogeneous concentration. The nucleation cell was loaded in a constant temperature bath and illuminated using a powerful lamp to observe the formation of nucleus. The time interval in which the first speck of particle formed in the supersaturated solution is noted and it is called the induction period (τ). The variations of induction period with supersaturation ratio for undoped and ferric sulfate doped KDP are presented in the figure 5. The results indicate that the induction period decreases as the supersaturation ratio increases for both the samples. The plots of $\ln \tau$ versus $1/(\ln S)^2$ for both the samples are given in the figure 6. From these plots, the values of the slope are obtained and the Gibbs free energy and interfacial tension are determined. Using the relevant equations, the critical nucleation parameters such as Gibbs free energy change (ΔG^*), radius of critical nucleus (r^*) and nucleation rate (J) were determined. The variations of Gibbs' free energy change, radius of critical nucleus and nucleation rate with supersaturation ratio for the samples are presented in the figures 7, 8 and 9. It is observed that the induction period decreases with increase of supersaturation ratio. From the results it is noticed that the nucleation parameters such as radius of critical nucleus, Gibbs' free energy change decrease with supersaturation ratio. The nucleation rate is observed to be increasing with the increase of supersaturation ratio. If the nucleation rate is low, the formation of multi-nuclei in the solution will be less and hence big-sized crystals could be grown. Interfacial energy at the solution-crystal interface is a crucial parameter involved in theories of nucleation and crystal growth. The value of interfacial energy is found to be 1.853×10^{-3} J / m^2 and 2.437×10^{-3} J / m^2 for undoped and ferric sulfate doped KDP samples respectively. The interfacial energy plays a vital role in the nucleation mechanism. The number of crystal nuclei produced per unit volume per unit time in the supersaturated solution is expressed as nucleation rate and the variables that affect the nucleation rate are pH, supersaturation, temperature and interfacial tension of the solution. Decrease in induction period is expected to increase the nucleation rate. The present study confirms that the evaluated nucleation parameters are feasible for the growth of bulk size single crystals [24, 25].

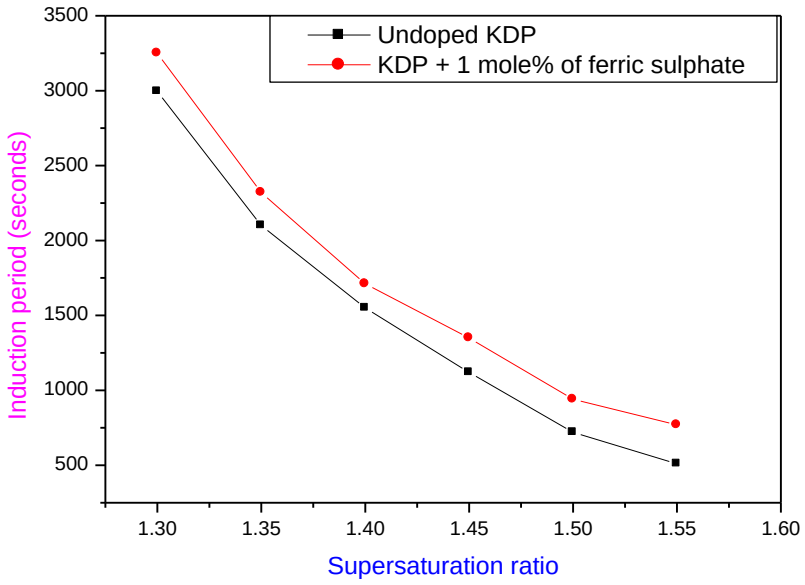

Figure 5: Variation of induction period with supersaturation ratio for undoped and ferric sulfate doped KDP samples

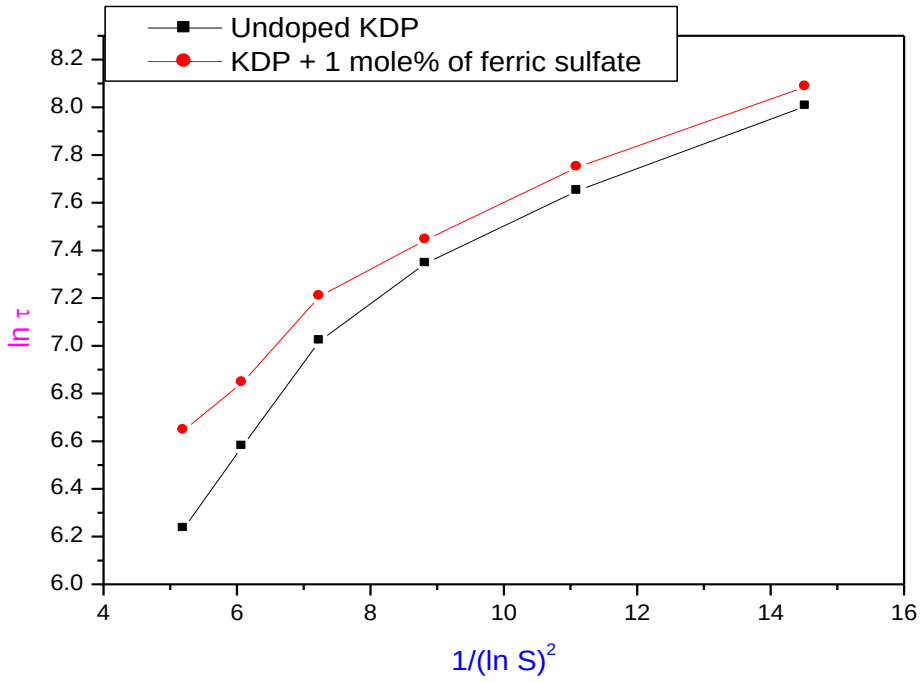

Figure 6: Plots of ln versus $1/(\ln S)^2$ for undoped and ferric sulfate doped KDP samples

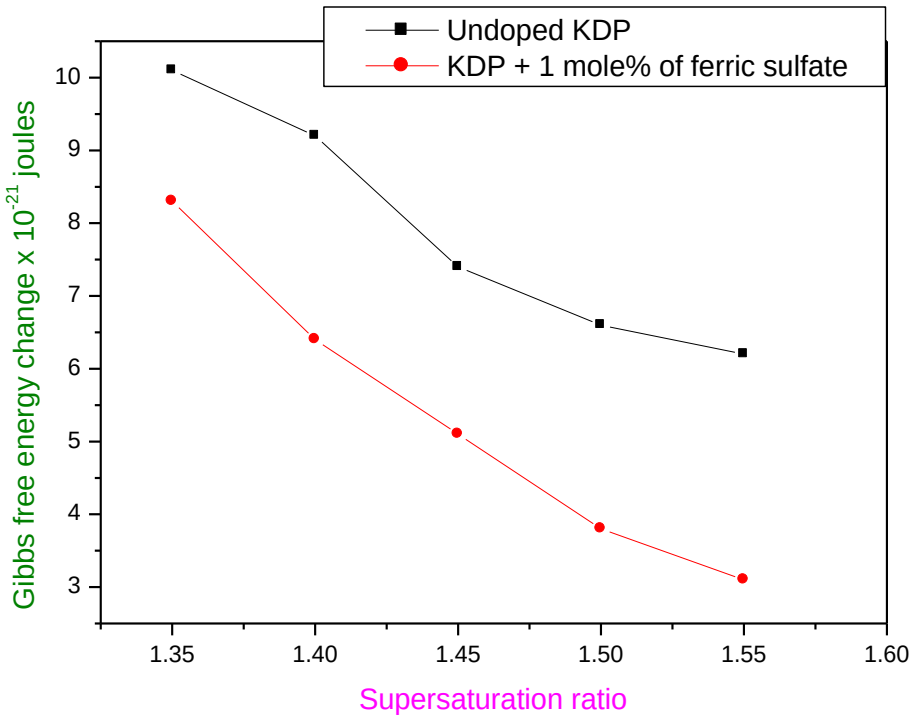

Figure 7: Variation of Gibbs free energy change with supersaturation ratio for undoped and ferric sulfate doped KDP samples

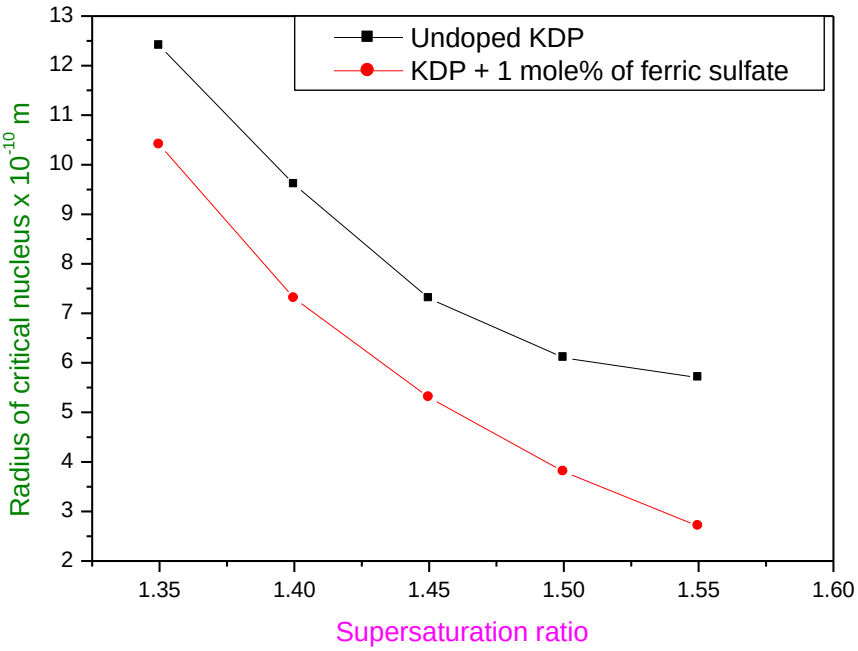

Figure 8: Variation of critical radius with supersaturation ratio for undoped and ferric sulfate doped KDP samples

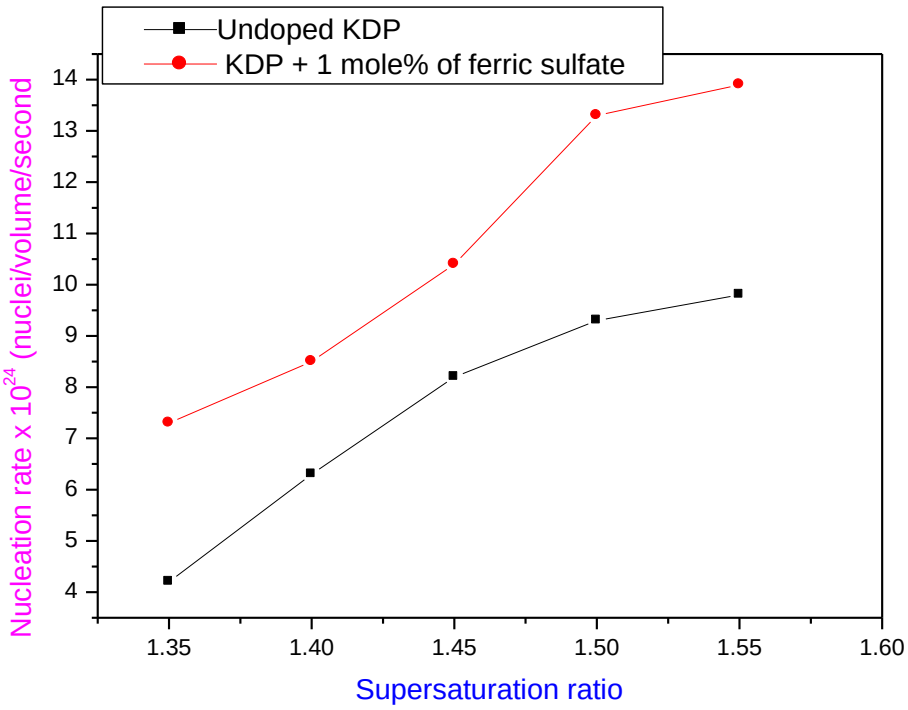

Figure 9: Variation of nucleation rate with supersaturation ratio for undoped and ferric sulfate doped KDP samples

3. Results and Discussions:

3.1 Structural Studies: The grown crystals undoped and ferric sulfate doped KDP were subjected to single crystal XRD studies to find the crystal structure and the lattice parameters. A single crystal X-Ray Diffractometer (Bruker-Nonius MACH3/CAD4) was used to obtain the single crystal XRD data of the grown crystals and the data are given in the table 1. From the data, it is ascertained that the crystal structure of undoped

and ferric sulfate doped KDP crystals is tetragonal. From the results, it is observed that the crystal unit cell parameters are slightly altered when KDP crystals are doped with ferric sulfate. KDP crystal is a ferroelectric crystal with the Curie temperature of 122 K and at room temperature it is in the paraelectric state. The samples crystallize in a non-centrosymmetric space group and hence these samples are both second order and third order NLO materials. The obtained lattice parameters are observed to be in good agreement with the reported values, JCPDS card No. 35-0807. [26].

Table 1: Values of axial and angular parameters for undoped and ferric sulfate doped KDP crystals

Sample	Unit cell parameters
Undoped`KDP crystal	a = b = 7.451(4) Å , c = 6.986 (6) Å , $\alpha = 90^o$, $\beta = 90^o$, $\gamma = 90^o$, V = 387.84 (2) $(Å)^3$
Crystal of KDP + 1 mole% of ferric sulfate	a = b = 7.458 (3) Å, c = 6.992(5) Å , $\alpha = 90^o$, $\beta = 90^o$, $\beta = 90^o$, V = 388.91(4) $(Å)^3$

3.2 Measurement of SHG Efficiency: The powder technique of Kurtz and Perry [27] with a pulsed Nd:YAG laser was used to measure the second harmonic generation (SHG) efficiency. The grown crystals were ground to powder of grain size 500-600 µm and subjected to measurement of SHG. From this technique, it is noticed that there is an emission of green radiation with a wavelength of 532 nm from the samples when the infrared laser light of 1064 nm (with a pulse width of 9 ns and repetition frequency of 10 Hz) is passed onto the powder samples. The second harmonic generation signal of 7.86 mJ for ferric sulfate doped KDP crystalline sample was obtained for an input energy of 0.70 J. But the standard KDP sample gave an SHG signal of 8.91 mJ for the same input energy. Hence, relative SHG efficiency of ferric sulfate doped KDP crystal is 0.882 times that of the undoped KDP sample. All the data in connection with SHG studies of the samples are given in the table 2. This test shows that the grown undoped and ferric sulfate doped KDP samples are the good second harmonic generators and both the samples have the non-centrosymmetric space group [28].

Table 2: Obtained data in connection with SHG studies for undoped and ferric sulfate doped KDP samples

S.No.	Sample Code / Name of the Sample	Output Energy (Milli Joule)	Input Energy (Joule)	Relative SHG Efficiency
1	Ferric sulfate doped KDP	7.86	0.70	0.882
2	KDP (Reference)	8.91	0.70	1

3.3 Hardness Parameters: Microhardness measurements were carried out for undoped and ferric sulfate doped KDP crystals using a Vickers microhardness tester. Here the grown crystals were subjected to microhardness test for different loads and indentation time given was 10s. For each load, several indentations were made and the diagonal indentation length was measured. Microhardness number (H_v) was determined using the relation $H_v = 1.8544\ P/d^2$ kg mm^{-2} where P is the load applied in kg and d is the average diagonal indentation length in mm [29]. Variation of microhardness number with applied load is presented in the figure 10. From the results of microhardness studies, it is observed that hardness number (H_v) increases with load for the grown crystals and this is due to reverse indentation size effect [30]. Hardness is found to be decreasing when ferric sulfate is added as dopant into KDP crystal. The addition of dopant into KDP crystal decreases the bond strength in the host material and hence hardness decreases. The plots of H_v versus d for undoped and ferric sulfate doped KDP crystals are shown in the figure 11. The results show that for both the samples, as d increases the H_v increases. Meyer's law [31] gives the relationship between load (P) and diagonal length (d) of indentation and it is given by $P=a\ d^n$. Here a and n are constants for a particular material. From the straight line graph of log P versus log d, the slope can be obtained. The slope is equal to the constant n which is called as Mayer's index number or work hardening coefficient. Plots of log P versus log d for the samples are displayed in the figures 12 and 13. The obtained values of work hardening coefficient are 2.794 and 3.026 respectively for undoped and ferric sulfate doped KDP crystals. Since these values are more than 1.6, the grown samples belong to the soft material category.

The nonlinear hardness behaviour of the crystals can be explained by Hays-Kendall's relation P= W + Ad2 where P is the applied load, d is the average diagonal indentation length, W is the minimum load to initiate plastic deformation in gram or resistance pressure, A is the load-independent constant [32]. The values of W and A are obtained from the plot drawn between P versus d^2 as shown in the figures 14 and 15. The obtained values of W are -23.510 g and -29.9183 g respectively for fundoped and ferric sulfate doped KDP crystals. Since these values are negative, the samples exhibit behaviour of reverse indentation size effect [33]. The corrected indentation size independent hardness (H_o) is determined using the relation $H_o=1.8544$ A. The evaluated value of H_o for undoped KDP crystal is 0.1339 g/μm^2 and value of H_o for ferric sulfate doped KDP crystal 0.1361 g/μm^2.

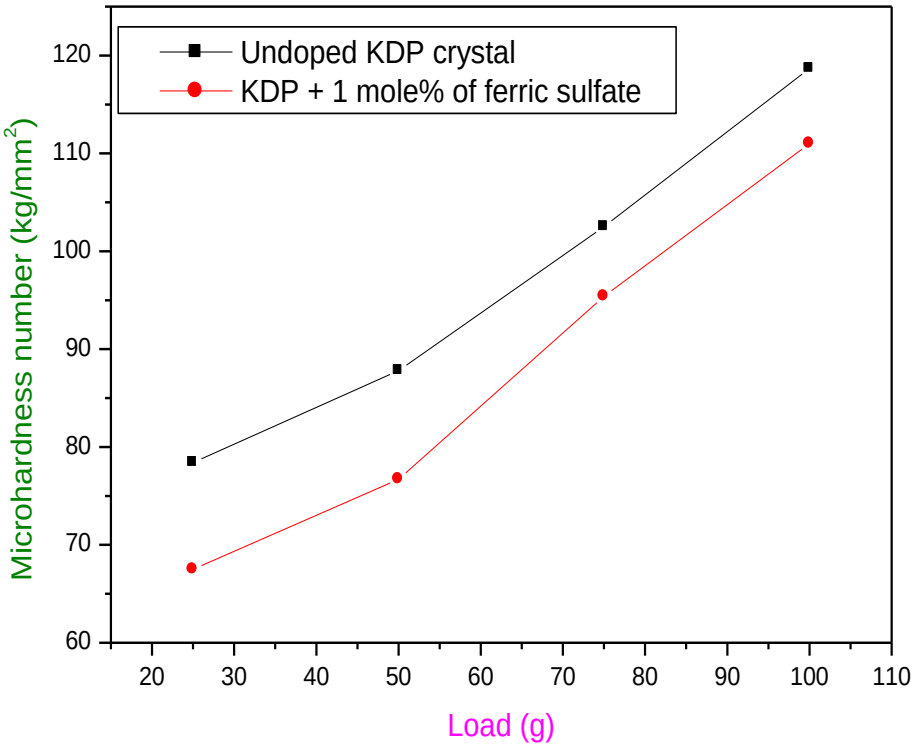

Figure 10: Plots of microhardness number versus the applied load for undoped and ferric sulfate doped KDP crystals

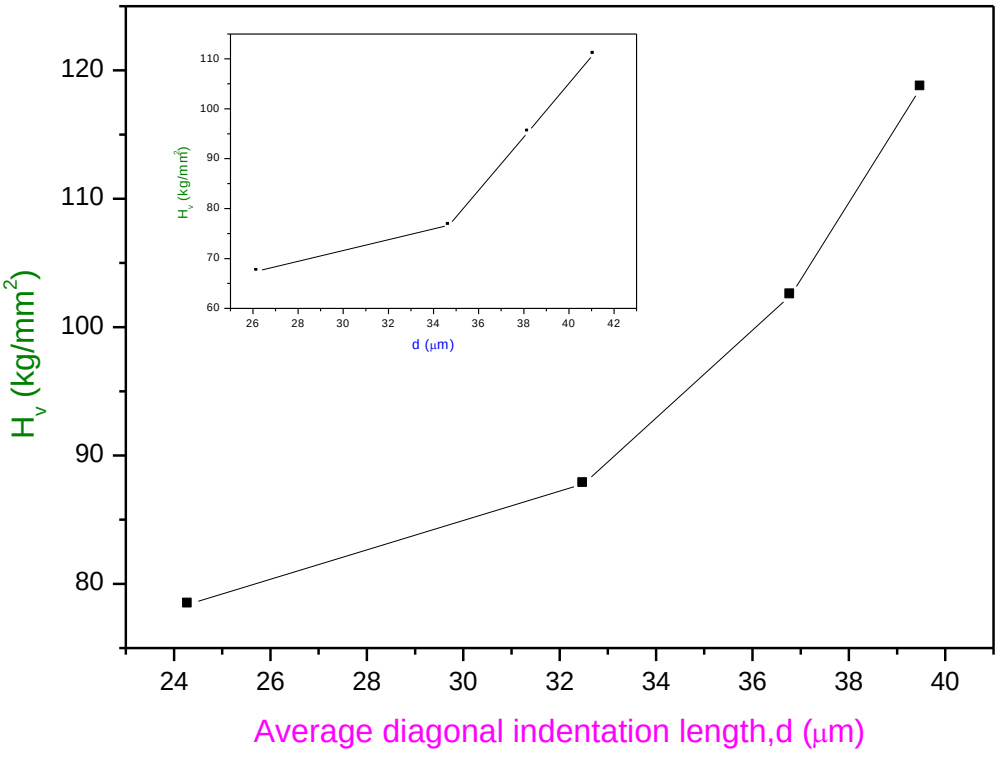

Figure 11: Plots of H_v versus d for undoped KDP crystal. Inset: Same plot for ferric sulfate doped KDP crystal

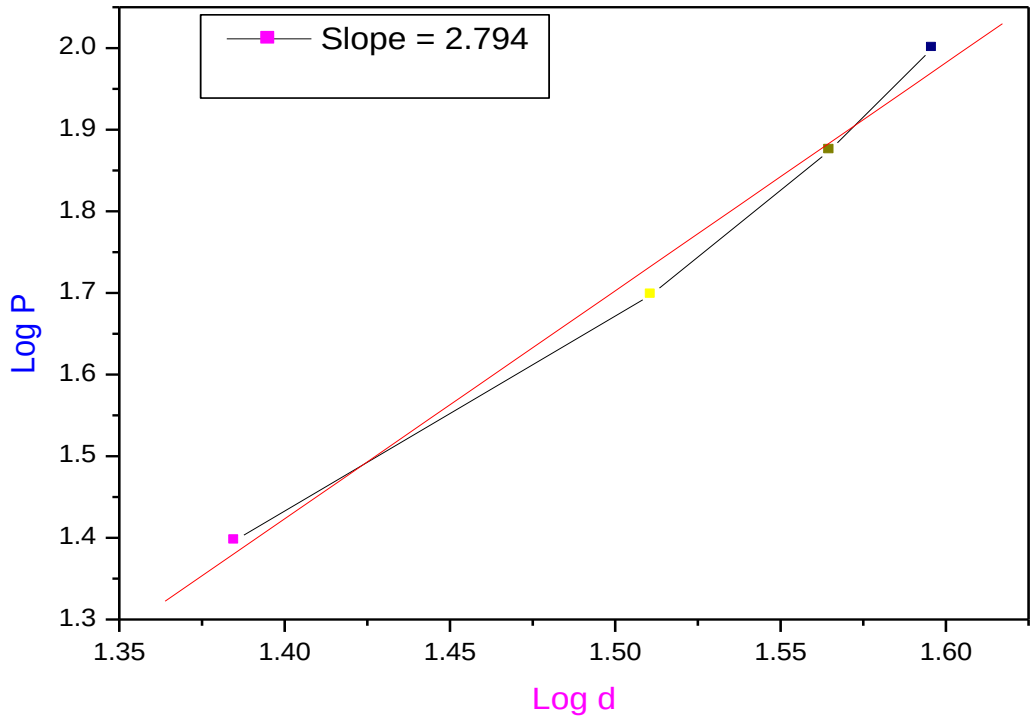

Figure 12: Plot of log (P) versus log (d) for undoped KDP crystal

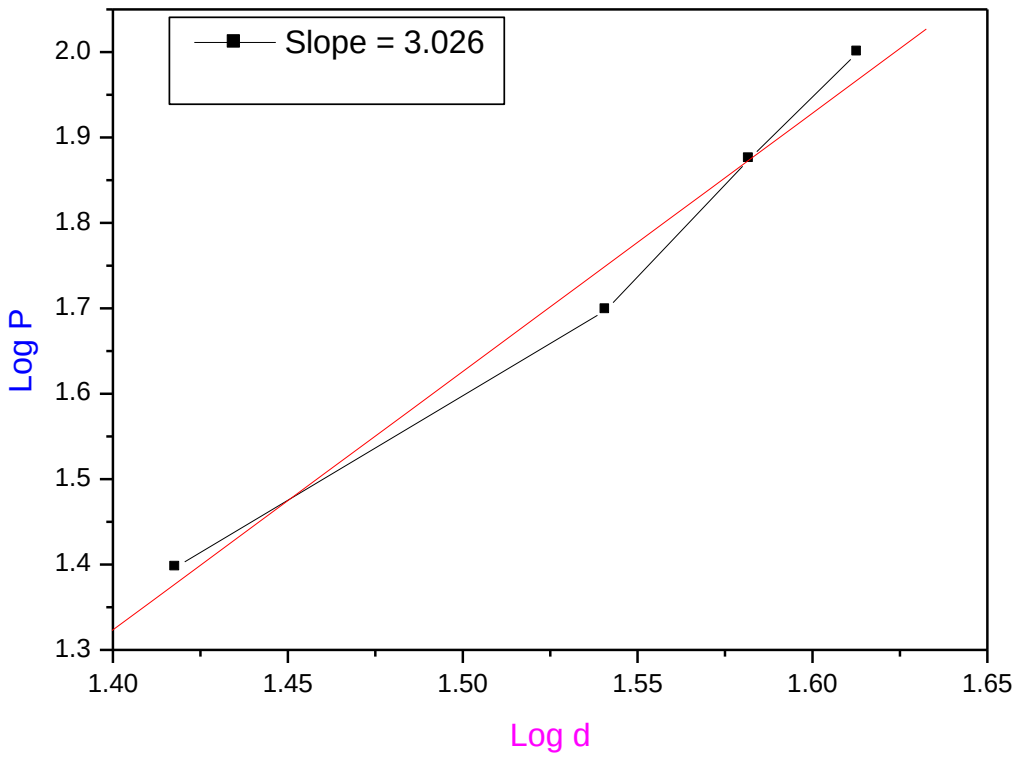

Figure 13: Plot of log (P) versus log (d) for ferric sulfate doped KDP crystal

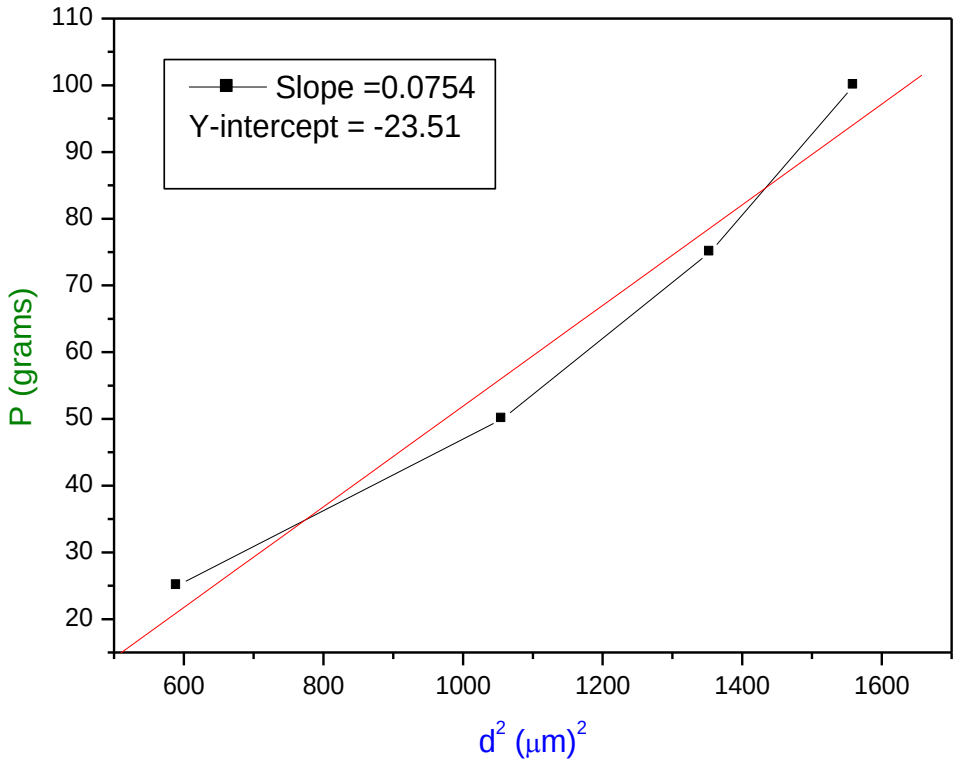

Figure 14: Plot of P versus d^2 for undoped KDP crystal

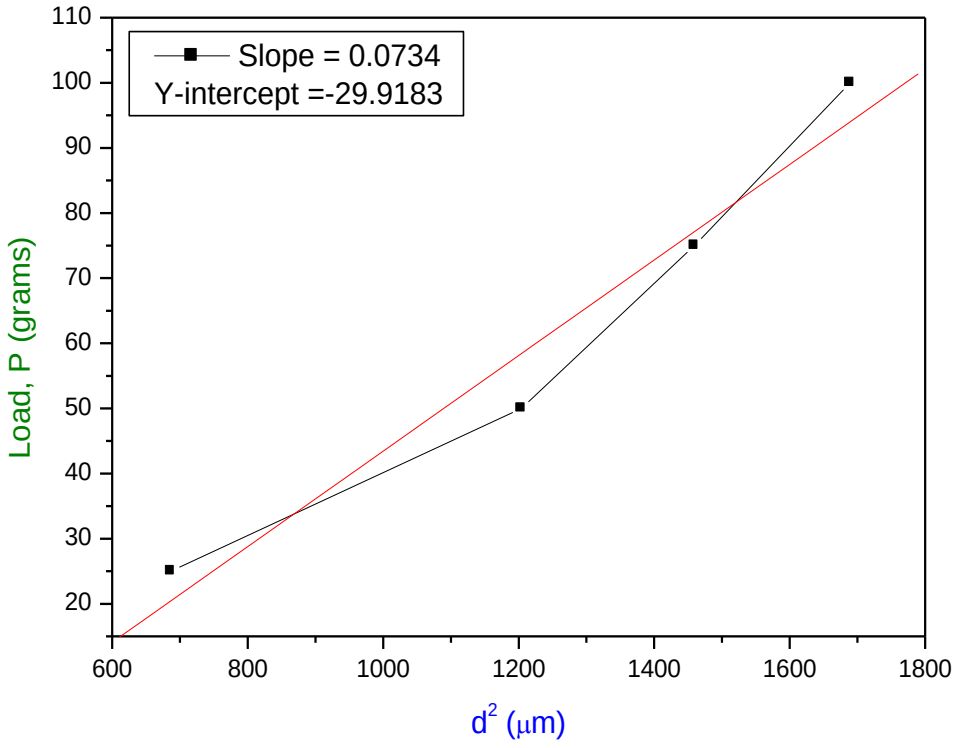

Figure 15: Plot of P versus d^2 for ferric sulfate doped KDP crystal

4. Conclusions:

Solubility and metastable zone width of undoped and ferric sulfate doped KDP crystals were measured. The samples are observed to have positive temperature coefficient of solubility. Induction period was measured for both the samples and it is decreases with the increase of supersaturation ratio and various critical nucleation parameters were determined. Growth of single crystals of undoped and ferric sulfate doped KDP crystals was carried out by slow evaporation technique and it is observed that there is a change of morphology, transparency and colour when KDP crystals are doped with ferric sulfate. XRD studies reveal the tetragonal structure of the samples. It is observed from the studies that hardness decreases when ferric sulfate was added as the dopant and this may be due to ferrous ions in the interstitial positions in the host KDP crystal. Hays-Kendall's approach was used to analyse the hardness properties. SHG efficiency of ferric sulfate doped KDP crystal was found to be less as compared to the undoped KDP crystal.

5. Acknowledgement:

The authors would like to thank the staff members of IIT, Chennai, St. Joseph's College, Trichy, Crescent Engineering College, Chennai, who helped to take the research data. We also thank the authorities of Aditanar College of Arts and Science, Tiruchendur and Manonmaniam Sundaranar University, Tirunelveli for the encouragement to carry out the research work.

6. References:

1. Masahiro Nakatsuka, Kana Fujioka, Tadashi Kanabe, Hisa-nori Fujita, J. Cry. Growth 171 (1997) 531-537.
2. N. Zaitseva, L. Carman, I. Smolsky, R. Torres, M. Yan, J. Cry. Growth 204 (1999) 512-524.
3. Y.N. Velikhov, I.M. Pritula, V.I. Salo, M.I. Kolybaeva, Inorg. Mater. 36 (7) (2000) 734.
4. Xun Sun, Xinguang Xu, Zhangshou Gao, Youjun Fu, Shen-glai Wang, Hong Zeng, Yiping Li, J. Cry. Growth 217 (2000) 404-409.
5. Shouji Hirota, Hideo Miki, Keisuke Fukui, Kouji Maeda, J. Cry. Growth 235 (2002) 541–546.
6. Selemani Seif, Kamala Bhat, Ashok K. Batra, Mohan D. Aggarwal, Ravindra B. Lal, Mat. Letters 58 (2004) 991-994.
7. I. Owczarek, K. Sangwal, J. Cry. Growth 102 (1990) 574.
8. A.A. Chernov, N.P. Zaitseva, L.N. Rashkovich, J.Crystal Growth 102 (1990) 793-800.
9. H.V. Alexandru, Crystal Research and Technology 30 (1995) 1071-1077.
10. I.V. Shnaidshtein, B.A. Strukov, S.V. Grabovskii, T.V. Pavlovskaya, L. Carman, Phys. Solid State 43 (12) (2001) 2276.
11. S.V. Grabovskii, I.V. Shnaidshtein, B.A. Strukov, Phys. Solid State 45 (3) (2003) 547.
12. J. Podder, J. Cryst. Growth 237–239 (2002) 70.
13. S. Hirota, H. Miki, K. Fukui, K. Maeda, J. Cryst. Growth 235 (2002) 541.
14. Y. Asakuma, et al. J. Mol. Struct. (Theochem.) 810 (2007) 7.
15. B. Wang, C.S. Fang, S.L. Wang, J. Crystal Growth 297 (2006) 352-355.
16. G.Z. Zheng, G.B. Su, X.X. Zhuang, Crystal Research and Technology 45 (2010) 145–148.
17. J.X. Ding, B. Liu, S.L. Wang, J. Inorganic Materials 26 (2011) 354-358.
18. G. Endert, M.L. Martin, Crystal Research and Technology 16 (1981) K65-K66.
19. G.Arunmozhi, De M. Gomes, E., Ganesamoorthy, S. Cryst. Res. and Technol. 2004, *39* (5), 408–413.
20. P.M. Ushasree, R. Muralidharan, R. Jayavel, P. Ramasamy J. Crystal Growth 210 (2000) 741-745.
21. D. Jayalakshmi,R. Sankar, R. Jayavel, J. Kumar, J. Crystal Growth 276 (2005) 243–246.
22. K. Selvaraju, K. Kirubavathi, N. Vijayan, S. Kumararaman J. Crystal Growth 310 (2008) 2859–2862.
23. A. Siva Dhas, P. Selvarajan, and T. H. Freeda, Materials and Manufacturing Processes, 24, 584–589, 2009.
24. M. Lydia Caroline, R. Sankar, R.M. Indirani, S. Vasudevan Mater. Chem. Phys.114 (2009) 490–494.
25. S. Dinakaran, J. Mary Linet, C. Justin Raj, S.M. Navis Priya, S. Jerome Das Materials Research Bulletin 43 (2008) 2010-2017.
26. K. Boopathi, P. Ramasamy, Opt. Mater. 37 (2014) 629–634.
27. S.K. Kurtz, T.T. Perry, J. Appl. Phys. 39 (1968) 3798.
28. Tun Z, Nelmes R J, Kuhs W F & Stansfield R F D, J Phys C: Solid State Phys. 21 (1988) 245-258.
29. S. Karan, S.P.S. Gupta, Mater. Sci. Eng. A 398 (2005) 198–203.
30. K. Sangwal, Mater. Chem. Phys. 63 (2000) 145–152.
31. Meyer,E, Verein,Z 1908, Duet. Ing. 52, 645.
32. C. Hays, E.G. Kendall, An analysis of Knoop microhardness, Metallography 6 (1973) 275–282.
33. Karuppasamy Pichan, Senthil Pandian Muthu, Ramasamy Perumalsamy J. Crystal Growth 473 (2017) 39–54.